CDF/ANAL/ELECTROWEAK/CDFR/9807
Version 2.0
June 22nd, 2009

Search for Diboson production in $WW/WZ \to l\nu jj$ using 3.9 fb^{-1}

Alberto Annovi[1]
INFN Frascati, Italy

Pierluigi Catastini[2]
Viviana Cavaliere[3]
Maria Agnese Ciocci[4]
Januscia Duchini[5]
University of Siena and INFN Pisa, Italy

Paolo Mastrandrea[6]
Fermilab

Marco Rescigno[7]
INFN and University of Rome, Italy

Anna Sfyrla[8]
University of Illinois

Abstract

We describe a search for $WW/WZ \to l\nu jj$ processes. A data sample of high p_T electrons and muons corresponding to approximately 3.9 fb^{-1} of integrated luminosity is used to reconstruct W boson. We look for another boson candidate in the event by selecting two additional jets. A fit to the invariant mass distribution M_{jj} of the two jets is performed. We found 1079 $\pm$ 232 (stat.) $\pm$ 86 (syst.) $WW/WZ \to l\nu jj$ events, corresponding to a statistical significance of 4.4σ. We also measure $\sigma_{WW/WZ} = 14.4 \pm 3.1(stat.) \pm 2.2(syst.)$.

[1]alberto.annovi@lnf.infn.it
[2]catasti@fnal.gov
[3]viviana@fnal.gov
[4]ciocci@fnal.gov
[5]januscia.duchini@pi.infn.it
[6]mastrand@fnal.gov
[7]rescigno@fnal.gov
[8]sfyrla@fnal.gov

1 Introduction

In this note we describe a search for WW/WZ production in the $l\nu jj$ final state using 3.9fb^{-1} of data collected by CDF.
CDF recently observed diboson production in the $\not\!\!E_T + jj$ channel using the *met* trigger [1]. On the other hand, in this analysis we attempt to reconstruct the $l\nu jj$ final states using a sample of high p_T electrons and muons. As a consequence, our analysis will not be sensitive to ZZ events, but we are sensitive to lower boson p_T.
Our strategy is quite straightforward. First select a sample of $W + njets$ with $n \geq 2$, then we reconstruct the dijet invariant mass from the two leading jets. Eventually, the dijet invariant mass is used as the main discriminant to separate the signal form the abundant background using a binned fit. This method does not optimized the discriminating power between signal and background, but it eventually minimises the systematics uncertainty and it is of straightforward interpretation.
At first, we will show the reconstruction and measurement of the inclusive $W \rightarrow l\nu$ cross-section to validate our samples. We will then focus on the $jet - jet$ candidate and show some distributions of data and Monte Carlo and the MC expectation of the number of signal events and the contribution of each background component. In section 9 we describe the fitting procedure to the M_{jj} and the results found on data. Finally, we describe the systematic uncertainties and our final results.

2 Data Sample

We use the high P_T electron and muon datasets up to period 21 for a total luminosity of 3.9 fb^{-1}.
For the electron decay channel we use the datasets bhelkd, bhelkh, bhelki, bhelmi, bhelmj, bhelmk and bhelmm selected using the ELECTRON_TRIGGER_18 trigger. For muon channel we use the datasets bhmukd, bhmukh, bhmuki, bhmumi, bhmumj, bhmumk and bhmumm. The events in these datasets are triggered by:

- CMUP: run $\leq$ 229763: MUON_CMUP_18_V || MUON_CMUP_18_L2_PT15V
- 229763 $<$ run: MUON_CMUP18_V
- CMX: run $\leq$ 200272: MUON_CMX18_V || MUON_CMX18_L2_PT15_V
- 200272 $<$ run $\leq$ 226194: MUON_CMX18_L2_PT15_V || MUON_CMX18_L2_PT15_LUMI_200_V
- 226194 $<$ run $\leq$ 257201: MUON_CMX18_&_JET10_V || MUON_CMX18_&_JET10_LUMI_270_V
- 257201 $<$ run: MUON_CMX18_V

Events have been reconstructed using version 6.1.4 of the offline software. We require the silicon to be fully operational using the Silicon Good Run List version 27 with logic (1,1,0,1) for electrons and (0,1,4,1) for muons.

3 Montecarlo Sample

The MonteCarlo samples are generated with Alpgen v2.10 prime and PYTHIA v. 6.325 for showering. Each sample is weighted to the same equivalent integrated luminosity according to:

$$weight = \frac{\int \mathcal{L} dt_{wanted} * \sigma_{ALPGEN}}{numberofevents}. \quad (1)$$

A list of the MC used for the analysis can be found in Table 1 - 2. Alpgen generates different samples for heavy flavour, Z+bb+Np and Z+cc+Np. In the light flavour sample Alpgen generates quark up, down, strange and charm without mass, while, during the showering, Pythia generates all five flavours with mass. It is then necessary to remove the double counting between the Z+Np sample that contains b's and c's from the Pythia showering and the heavy flavour sample.
A way to handle this overlap is to remove events that have jets that come from a b or a c quark with a bottom or charm hadron inside the cone of the jet (0.4 in our case) in the light sample. Then, we take the c sample and remove events that have jets with a b inside the cone of the jet. We don't have to remove anything from the b sample because a cut in the P_T of the jet removes all the charm. After this procedure we can simply add all the samples togheter.

4 $W \rightarrow e\nu$ selection

$W \rightarrow e\nu$ events are selected looking for one tight electron that satisfies the requirements of Tab. 3 and $\not\!\!E_T > 25\ GeV$. Moreover, $\not\!\!E_T$ is corrected for loose muons in the event and for jets with $E_{Traw} > 8\ GeV$ (the raw jet energy is replaced with the level 5 corrected one). Finally, to reconstruct the W we also require the trasverse mass of the W ($M_T(W)$) to be $> 30\ GeV/c^2$.

4.1 Electron Energy Scale

The electron energy scale is already corrected in Topntuple. However we still observe a shift in the mass peak (Fig.1). For this reason, we correct the energy of the electrons to match the measured Z boson mass peaks at 91 GeV/c^2 . Since we have a slightly different selection from other analysis we have to calculate our own scale factors using the following expressions (see [2]):

$$E^{CEM}_{scale} = \frac{91}{M_{CC}} \quad (2)$$

The value of M_{CC} is obtained from a gaussian fit to the mass peak in both data and MC performed between 86 and 98 GeV/c^2 (Fig.2).
We obtain a scale factor of 1.005 for data and 0.995 for MC.

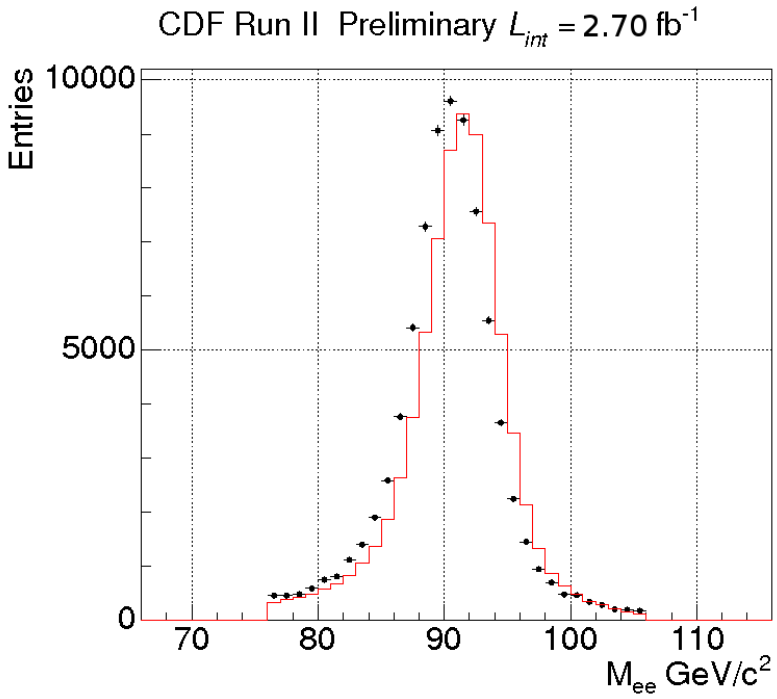

Figure 1: M_{ee} in data (dot) and MC (histogram).

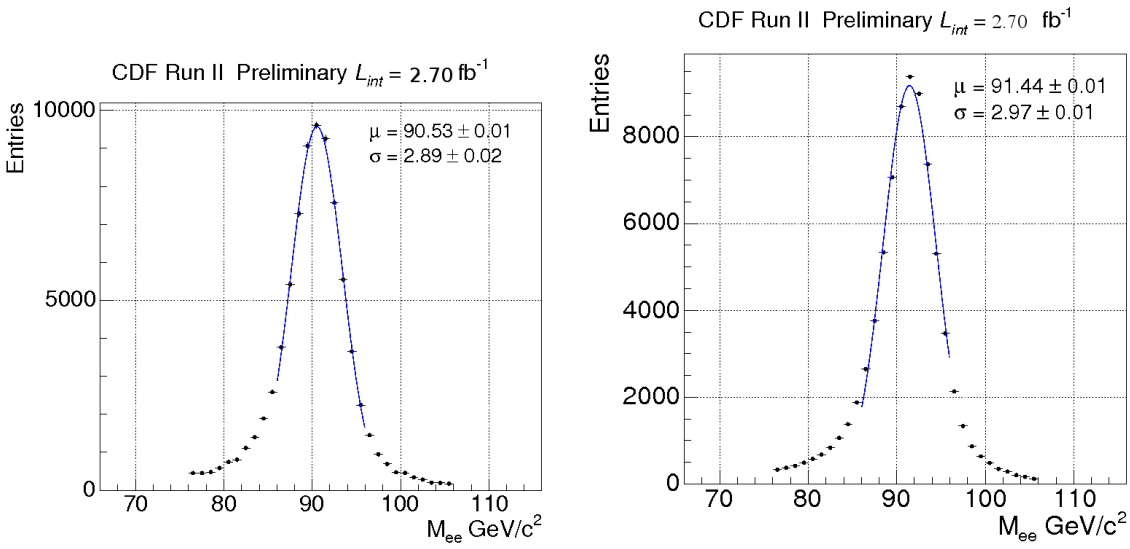

Figure 2: Fit to the M_{ee} for tight electrons in MC (left) and data (right)

sample	σ_{gen}	Ngen
Diboson		
itopww	12.40	2284862
itopwz	3.70	2306591
itopzz	3.80	2323812
W $(e\nu)$+jets		
ptopw0	1800	4928812
ptopw1	225	4909767
ptop2w	35.30	1003193
ptop3w	5.59	1003040
ptop4w	1.03	989607
W $(\mu\nu)$+jets		
ptopw5	1800	5017218
ptopw6	225	5003166
ptop7w	35.3	1002804
ptop8w	5.59	1013373
ptop9w	1.03	988545
W $(\tau\nu)$+jets		
utopw0	1800	4885557
utopw1	225	4987134
utop2w	35.3	923989
utop3w	5.59	1008221
utop4w	1.03	186494
W+HF		
btop0w	2.98	1542539
btop1w	0.888	1545970
btop2w	0.287	1498550
btop5w	2.98	1524880
btop6w	0.888	1508029
btop7w	0.287	1506613
ctop0w	5.	2008023
ctop1w	1.79	1987389
ctop2w	0.628	1926322
ctop5w	5.	1985033
ctop6w	1.79	1979810
ctop7w	0.628	1970504
top		
ttkt75	6.7000	5445003

sample	σ_{gen}	Ngen
Z(e^+e^-)+jets		
ztopp0	158.	2639520
ztopp1	21.60	2630345
ztop2p	3.47	536159
ztopzb	3.46	4641816
ztop3p	0.55	528491
ztop4p	0.0992	525065
Z$(\mu^+\mu^-)$+jets		
ztopp5	158	2665104
ztopp6	21.60	2664729
ztop7p	3.47	530843
ztopzt	3.46	4710842
ztop8p	0.548	536159
ztop9p	0.0992	536159
Z+HF		
ztopb0	0.511	516239
ztopb1	0.134	493381
ztopb2	0.0385	498736
ztopb5	0.511	437329
ztopb6	0.134	494480
ztopb7	0.0385	478485
ztopc0	1.08	662939
ztopc1	0.331	695289
ztopc2	0.107	658211
ztopc5	1.08	671375
ztopc6	0.331	663431
ztopc7	0.107	705108
Z$(\tau^+\tau^-)$+jets		
ztopt3	158.	5860164
ztopt4	21.5	5864300
ztopt2	4.14	2273221
xtopt0	160	1136851
xtopt1	8.3	1153959
xtopt2	1.82	2270345
zttt0h	4.07	268428
zttt1h	0.707	268428
zttt2h	0.117	263291
zttt3h	0.0185	268428
zttt4h	0.0033	56398

Table 1: List of the Monte Carlo samples.

Sample	σ_{gen}	Ngen
DY		
DY		
xtop0p	160.0000	536159
xtop1p	8.3900	515515
xtop2p	1.6100	536159
xtoppb	1.6000	4610071
xtop3p	0.2330	525670
xtop4p	0.0398	520758
xtop5p	160.0000	524357
xtop6p	8.3900	530696
xtop7p	1.6100	525769
xtoppc	1.6000	4644940
xtop8p	0.2330	524697
xtop9p	0.0398	529635

Sample	σ_{gen}	Ngen
DY		
ytop0p	4.0700	519104
ytop1p	0.7060	524895
ytop2p	0.1170	513428
ytop3p	0.0185	531075
ytop4p	0.0033	527280
ytop5p	4.0700	536159
ytop6p	0.7060	529581
ytop7p	0.1170	531006
ytop8p	0.0185	520531
ytop9p	0.0033	527838

Table 2: List of the Monte Carlo samples.

Variable	Cut
Region	central
Track	yes
Iso/E_T	≤ 0.1
E_T	> 20 GeV
P_T	> 10 GeV
Track $\lvert Z_0 \rvert$	≤ 60cm
E/P	≤ 2 (unless $p_t \geq 50$ GeV/c)
Had/Em	$\leq 0.055 + 0.00043 \cdot E$
Signed CES ΔX	$3.0 \leq q\Delta X \leq 1.5$
CES ΔX	< 3cm
Lshr	< 0.2
CES Strip χ^2	$\leq$10
Fiducial	yes

Table 3: Electron selections.

Variable	Cut
Iso/P_T	≤ 0.1
P_T	> 20 GeV
Track $\lvert Z_0 \rvert$	≤ 60cm
CMU Fid	$x - fid < 0$cm, $z - fid < 0$cm
CMP FId	$x - fid < 0$cm, $z - fid < -3$cm
CMX Fid	$x - fid < 0$cm, $z - fid < -3$cm
E_{em}	$\leq 2 + max(0, (p - 100) \cdot 0.0115)$
E_{had}	$\leq 6 + max(0, (p - 100) \cdot 0.028)$
COT Ax hits / Ax Seg	$\geq 5 / \geq 3$
COT Ax hits / Ax Seg	$\geq 5 / \geq 3$
Track no si hits $\lvert d_0 \rvert$	< 0.2cm
Track si hits $\lvert d_0 \rvert$	< 0.02cm
ρ_{exit}	> 140 if CMX
$\lvert \Delta X_{CMU} \rvert$	≤ 7cm
$\lvert \Delta X_{CMP} \rvert$	≤ 5cm
$\lvert \Delta X_{CMX} \rvert$	≤ 6cm
No muons in bluebeam	run <154449
No muons in keystone	run <186598
No muons in miniskirt	run <186598
Larry corrections	data only

Table 4: Muon selections.

5 $W \to \mu\nu$ selection

We reconstruct CMUP and CMX muons separately according to the selection of Table 4. We also correct $\not\!\!E_T$ for loose muons and jet with $E_{Traw} > 8\,GeV$ (Level 5 correction). Moreover, we also require the $M_T(W) > 30\ GeV/c^2$.

6 Background

We consider the following backgrounds both for inclusive W and Di-Boson reconstruction:

- $W \rightarrow l\nu$ + n jets ; $n \geq 0$, $l = e, \mu, \tau$
- $Z \rightarrow ll$ + n jets ; $n \geq 0$, $l = e, \mu, \tau$
- $t\bar{t}$
- QCD

The only background that is not extracted by Monte Carlo is the QCD contribution. The other sources are estimated by the MC of Table 1 - 2.
QCD background is estimated using the technique described in [3] [4]. A fit to the $\not\!\!E_T$ distribution in the range [0,200] GeV is performed both in the inclusive and the di-jet cases (see Fig.3 for an example in the di-jet case, with selections described in section 8). In the muon sample, the QCD template is extracted from the high isolation sample ($Iso > 0.2$), while in the case of the electron samples we use the antielectron method. For all the other background contributions the template is extracted from Monte Carlo.

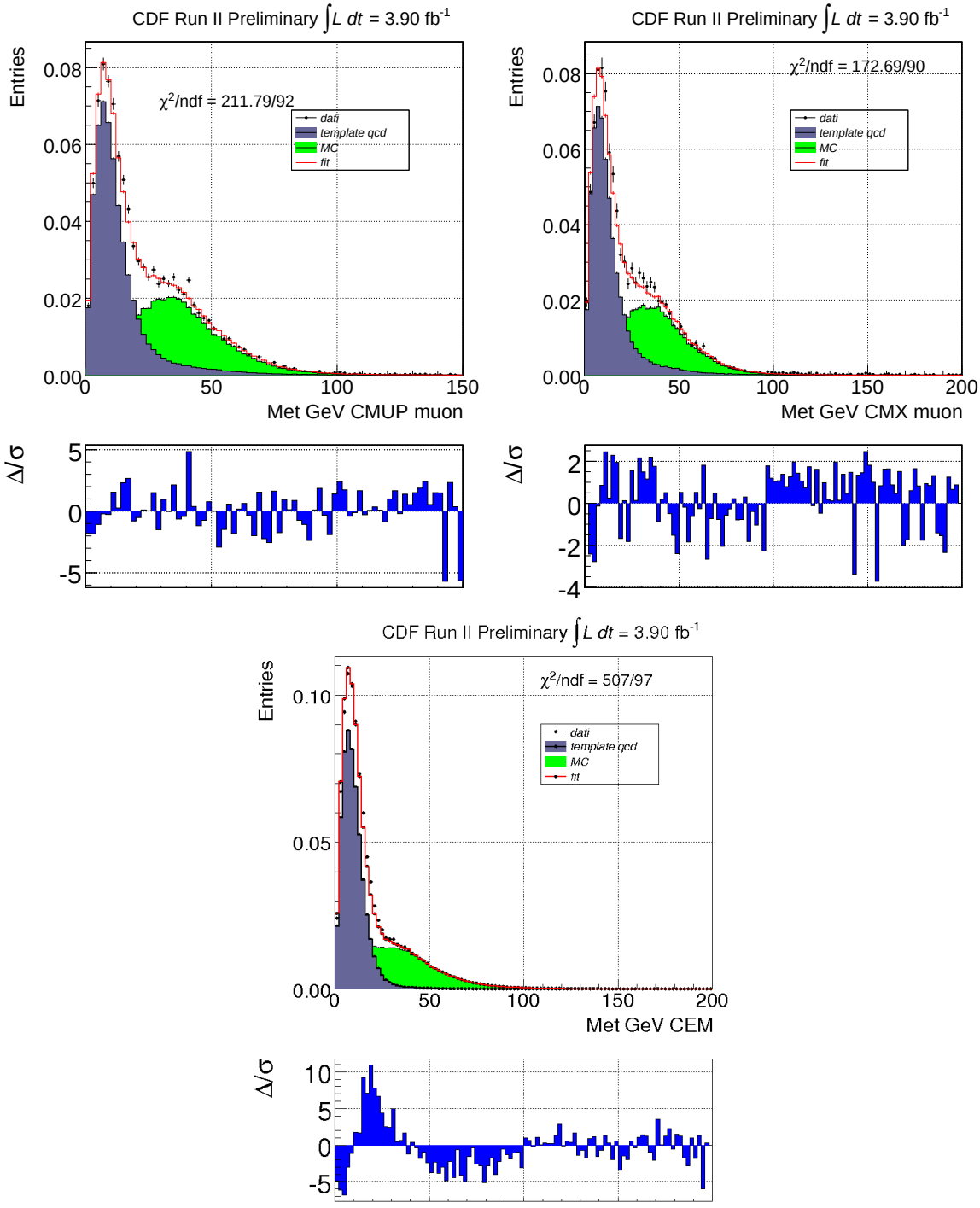

Figure 3: Upper left: $\not\!\!E_T$ fit of the QCD background for CMUP. Upper right: $\not\!\!E_T$ fit of the QCD background for CMX. Bottom: $\not\!\!E_T$ fit of the QCD background for CEM. These fits refere to the di-jet selection.

7 Inclusive $W \to l\nu$ Results

Our inclusive study is based on 2.7 fb^{-1} of integrated luminosity, that is of course a large subsample of the sample used in our main analysis.
In Tab. 5 we show the estimated number of events for the W inclusive sample. The resulting cross section is also shown and is in good agreement with the CDF measurement [5].
Fig. 4 - Fig. 9 show the distributions of some kinematical variables for CEM, CMUP and CMX samples. An overall reasonable agreement between data and MC is observed.

Sample	**CEM**	**CMUP**	**CMX**
MC W +jets	1426100 ± 85667	680890 ± 40853	427846 ± 25670
MC Z+jets	12824 ± 255	79275 ± 423	47386 ± 217
MC Z(tau)	1835 ± 184	849 ± 171	520 ± 23
diboson	1754 ± 42	932 ± 31	507 ± 23
top	919 ± 30	542 ± 23	248 ± 16
QCD (from data)	58029 ± 2337	9693 ± 522	7465 ± 417
MC all	1538640	790060	494697
data	1532320 ± 1237	801395 ± 895	503529 ± 710
W Cross Section	2.68 nb	2.87 nb	2.75 nb

Table 5: Inclusive $W \to l\nu$ results.

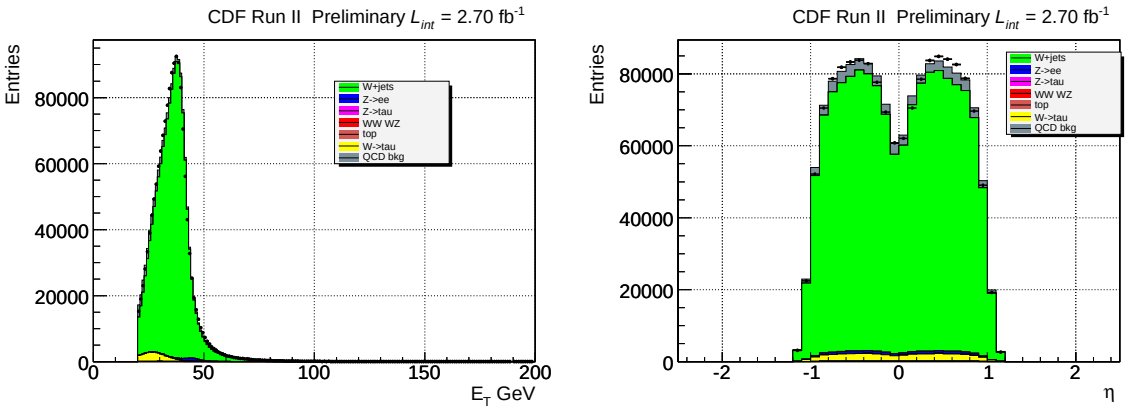

Figure 4: Left: electron E_T; right: electron η.

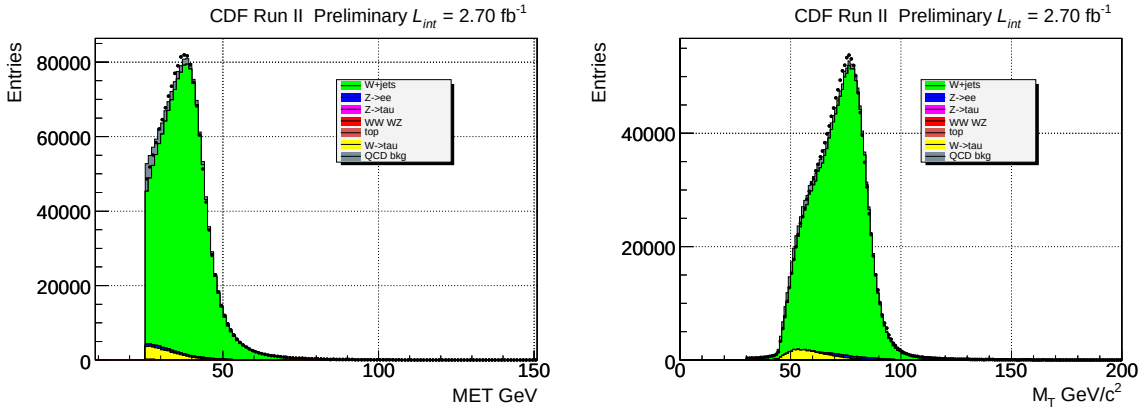

Figure 5: Left: electron $\not\!\!E_T$; right: $M_T W \to e\nu$.

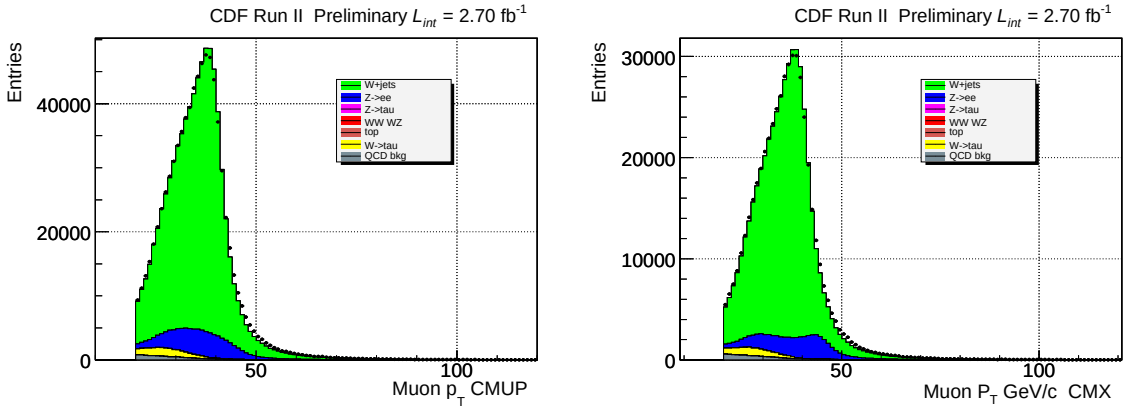

Figure 6: Left: CMUP P_T; right: CMX P_T.

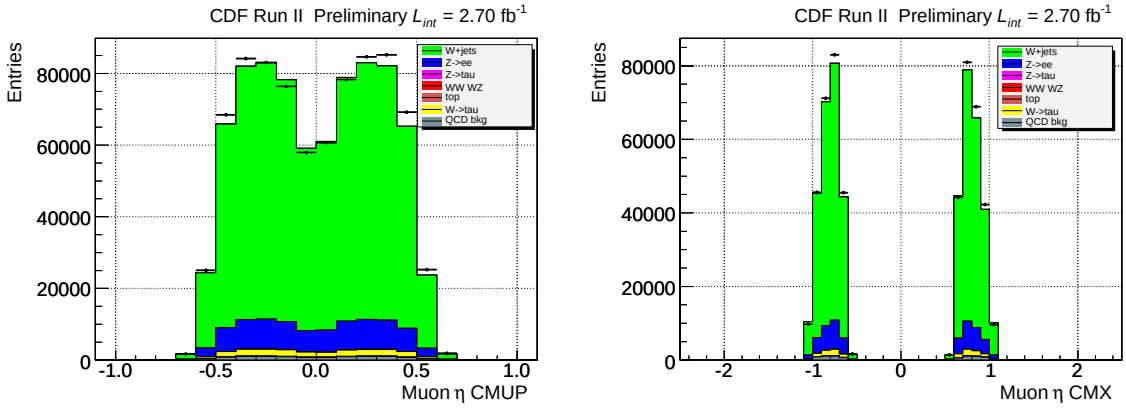

Figure 7: Left: CMUP η; right: CMX η.

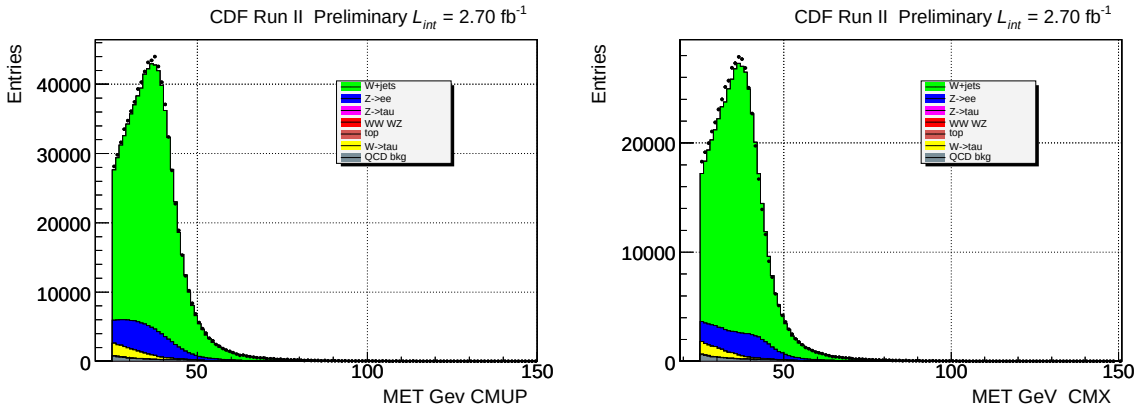

Figure 8: Left: CMUP $\not\!\!E_T$; right: CMX $\not\!\!E_T$.

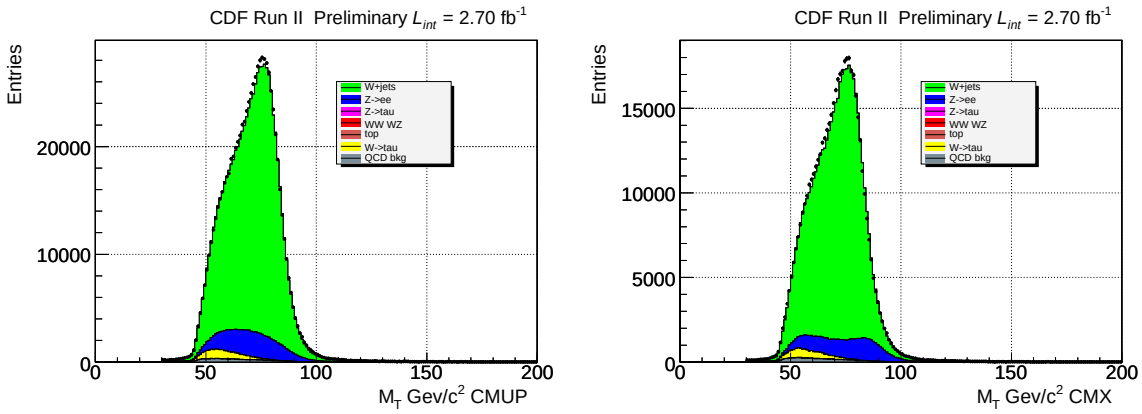

Figure 9: Left: CMUP $M_T W \to \mu\nu$; right: CMX $M_T W \to \mu\nu$.

8 Jet-Jet Candidate Selection and Expected Yields

To selected our di-Boson candidates sample we require at least two jets. The jets are reconstructed using JETCLU04 and corrected at level 7; in addition they are required to have $E_T > 20\ GeV$, $|\eta| < 2.4$ and $\Delta\eta_{j1j2} < 2.5$.
In what follow, when we refere to muon sample we consider CMUP and CMX samples together and when we refere to the electron sample we consider CEM sample. In addition, we apply a selection cut on the p_T of the W/Z jet-jet candidate. We require $p_T > 40\ GeV/c$ for the hadronic diboson. As shown in Fig.10 a clear step is observed (both in muons and electrons) for $p_T \approx 40\ GeV$. This is a consequence of our jet selection that, in the case of boosted hadronic W/Z, reaches full acceptance at $40 GeV/c$. For values above the cut a steep and smooth decreasing shape is present.
The effect of the $p_T > 40\ GeV/c$ cut on the M_{jj} distribution is shown in Fig.11 and Fig.12: in the M_{jj} distribution for $p_T > 40\ GeV$ the signal is expect to lay on the smooth decay of the background distribution (right), an eventual bump can be observed also by eye and a good agreement between the MC expectation and data is observed both for electrons and muons for $M_{jj} > 36\ GeV$; on the other hand the agreement between data and MC is less good for the $p_T < 40\ GeV/c$ case, in addition the signal is expected to lay near the turn on shoulder of the background.
For these reasons, at the moment in our analysis we decide to consider the $p_T > 40$ GeV/c subsample only since we believe that the $p_T < 40\ GeV/c$ requires more careful understanding. In any case we consider rather essential to treat separately the two samples since they correspond to two different kinematical regimes. In fact, if these samples are treated together, we must assume that the p_T distribution of the hadronic W/Z candidates ($P_T(jj)$) is correctly reproduced by of background model (in contrast with what shown in Fig.10). This happens even if the M_{jj} distribution without the $P_T(jj)$ cut seems to be in reasonable agreement between data and Monte Carlo (Fig.13)

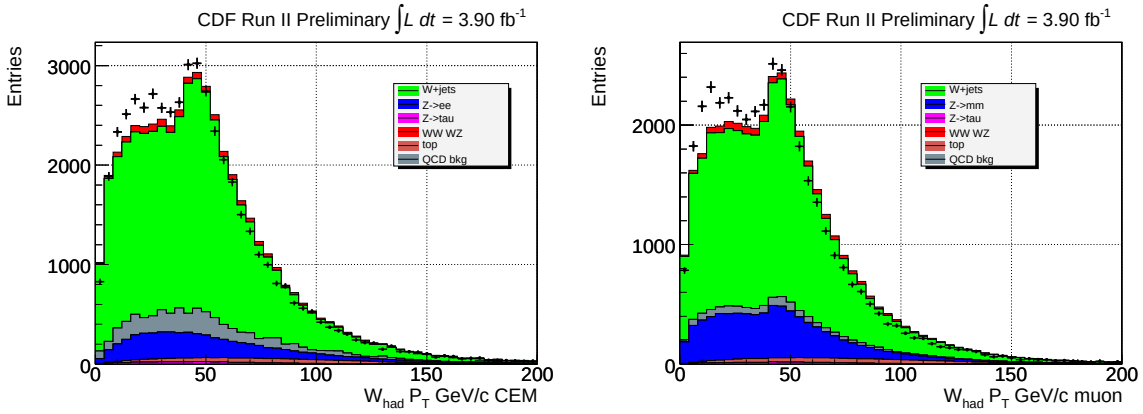

Figure 10: p_T distribution of the $W/Z \rightarrow jetjet$ candidate; left: CEM sample; right: CMUP + CMX sample.

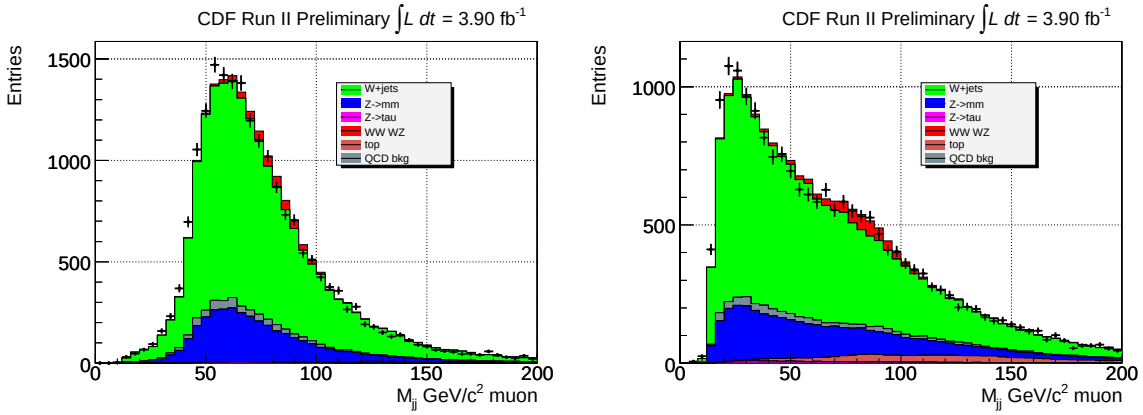

Figure 11: M_{jj} distribution in the CMUP + CMX sample with $p_T(jj) < 40GeV/c$ (left) and $p_T(jj) > 40GeV/c$ (right).

In Tab. 6 we show the estimated number of events for the di-Boson sample. Fig.14 - Fig.17 show the distributions of some kinematical variables for CEM, CMUP and CMX samples. An overall reasonable agreement between data and MC is observed.

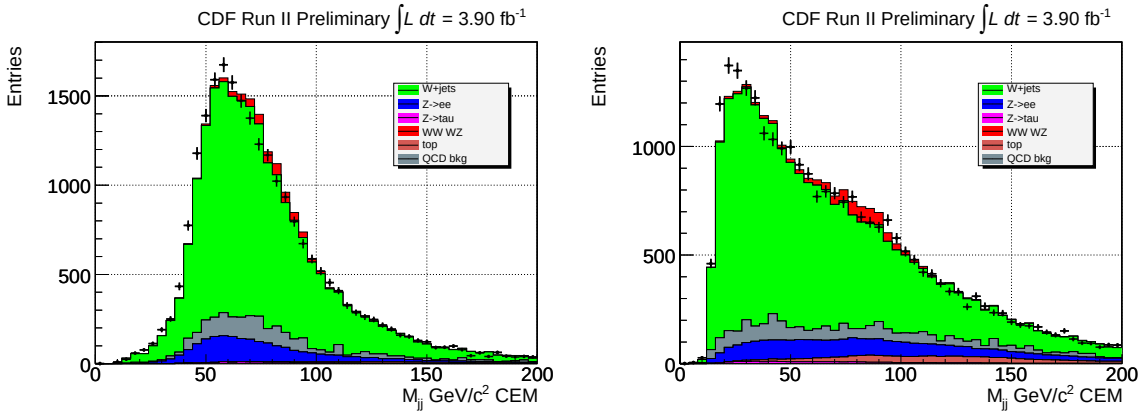

Figure 12: M_{jj} distribution in the CEM sample with $p_T(jj) < 40GeV/c$ (left) and $p_T(jj) > 40GeV/c$ (right).

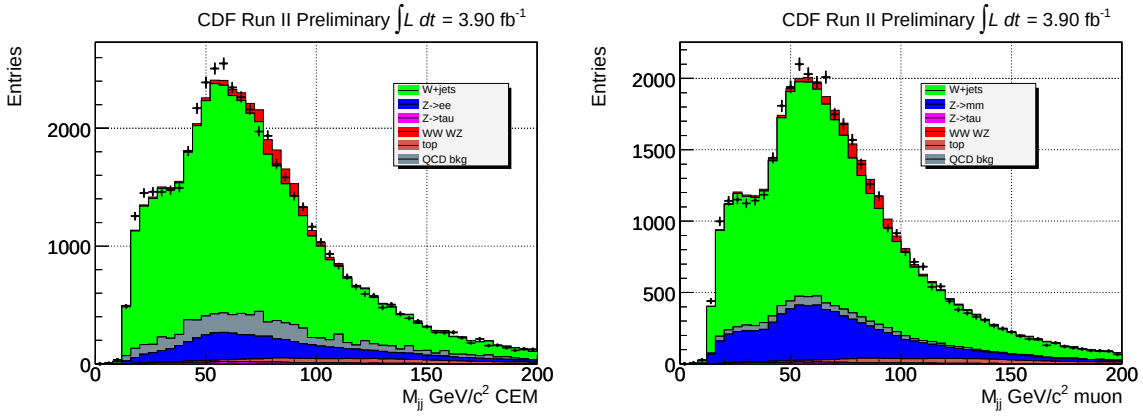

Figure 13: M_{jj} distribution without the $p_T(jj) > 40GeV/c$ cut; left: CEM; right: CMUP + CMX.

Sample	**CEM**	**CMUP + CMX**
MC W +jets	19245 ± 1520	13371 ± 1069
MC Z+jets	2553 ± 70	3504 ± 87
diboson	725 ± 30	579 ± 27
top	878 ± 32	745 ± 28
QCD (from data)	2054 ± 204	755 ± 73
Total MC + QCD	25455	18954
data	25684 ± 160	18891 ± 137

Table 6: MC estimate of the expected number of events for signal and each background component for $M_{jj} \in$ [0,200] GeV/c^2.

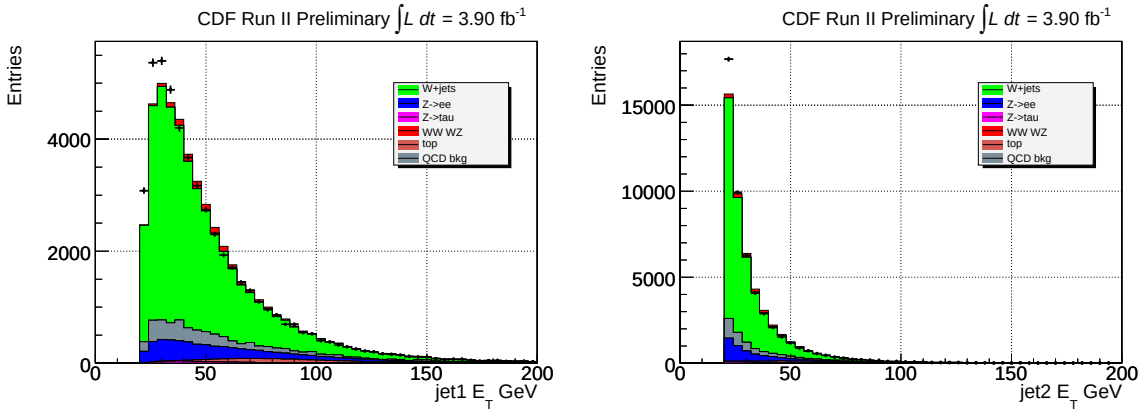

Figure 14: CEM. Left: leading jet E_T; right: second jet E_T.

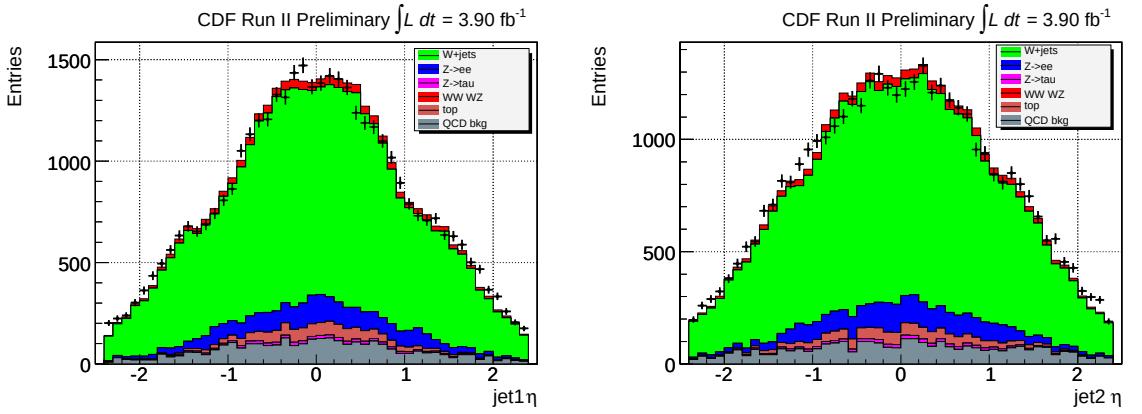

Figure 15: CEM. Left: leading jet η; right: second jet η.

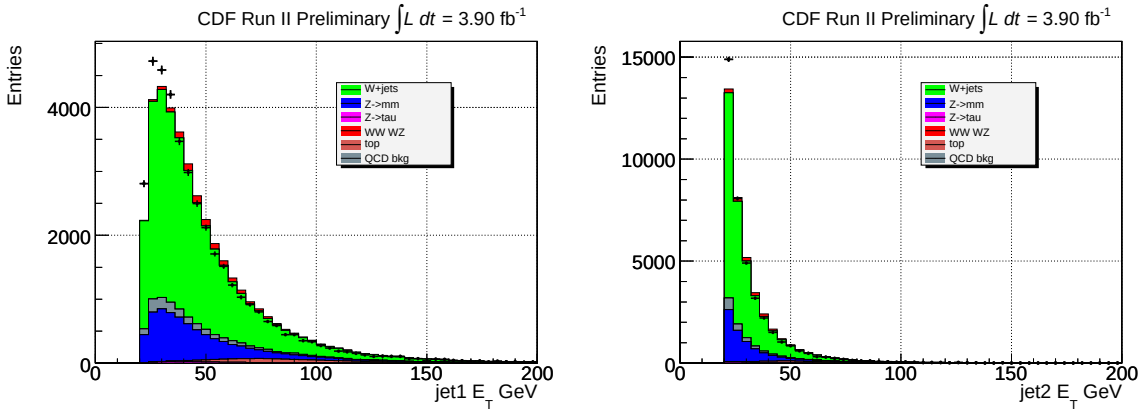

Figure 16: CMUP+CMX. Left: leading jet E_T; right: second jet E_T.

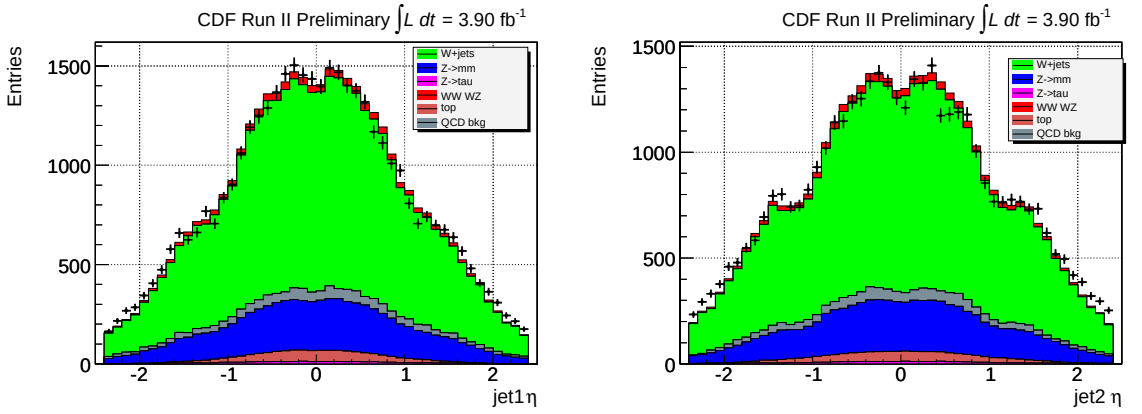

Figure 17: CMUP+CMX. Left: leading jet η; right: second jet η.

9 Fitting Procedure to the Dijet Mass Distribution

The WW/WZ signal is extracted perfoming a χ^2 fit of the M_{jj} distribution; the χ^2 minimisation is perfromed using MINUIT.
As templates for the fit we consider three components: the Electroweak background, the QCD background and the signal.
In particular, we perform a separate fit for the electron and the muon channels: we believe that our choice ensures a more straightforward cross-check of the two samples separately and avoids the uncertainty in the combination of the two sample templates, i.e. we do not have to combine the template of each component on purely MC driven assumptions; in this way, the contribution of each component for each decay channel is determined by the fit.
The fits are perfromed in the mass range [36,200] GeV/c^2 and the statistics uncertainty on the templates (weighted histograms) is included in the fit as described in [6]. The total number of events is a free parameter of the fit.

9.1 Electroweak Background

As electroweak background we consider:

- $W \rightarrow l\nu$ + n jets ; $n \geq 0$, $l = e, \mu, \tau$
- $Z \rightarrow ll$ + n jets ; $n \geq 0$, $l = e, \mu, \tau$
- $t\bar{t}$

each single contribution to the M_{jj} shape is extracted by Monte Carlo (see Section 3) and added together in what we consider our EWK template. The relative contribution of each component is determined and fixed by MC. As shown in Fig.14 and Fig.16 the dominant contribution comes from $W + jets$ both for electrons and muons.
Fig.18 shows the resulting template for the electrons (left) and muons (right).

The total EWK contribution is a free parameter to be determined by the fit.

9.2 QCD Background Template

In the case of the electron sample, the QCD M_{jj} template is extracted using the antielectron method; for the muon sample, we select a sample of non isolated muons; the method is described in [3] [4].
The resulting tempaltes are shown in Fig.19 for electrons (left) and muons (right).

The QCD content estimated in section 6 is rescaled to the expected number of events in our M_{jj} fit region after the cuts on the $\not\!\!E_T > 25 GeV/c^2$ and $M_T(W \rightarrow l\nu) > 30 GeV/c^2$ are applied.
In the M_{jj} fit the QCD component is gaussian-constrained to this rescaled value with a width of 20%, i.e. conservatively twice the error returned by the fit of section 6.

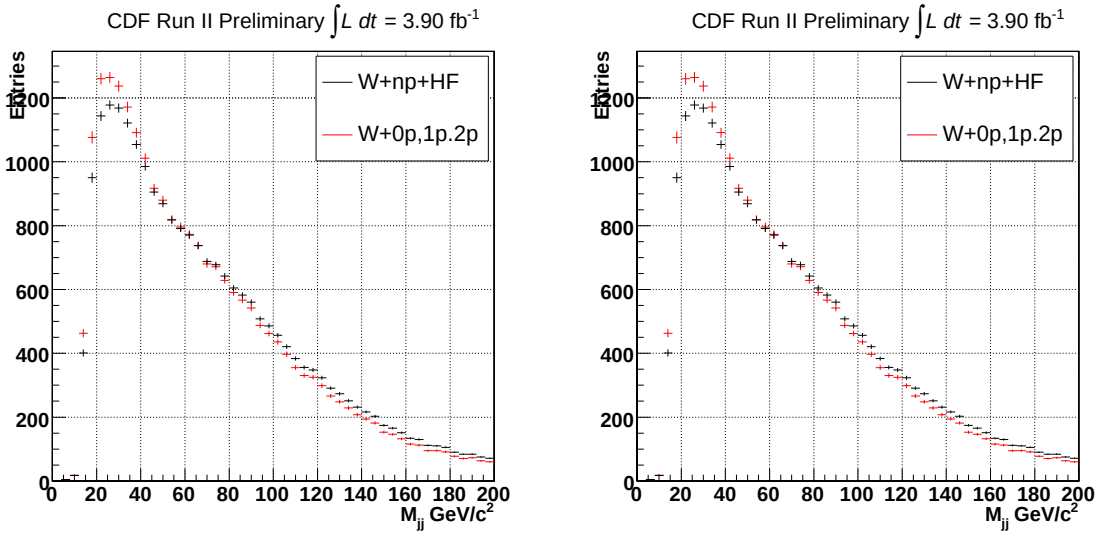

Figure 18: EWK M_{jj} template for electrons (left) and muons (right).

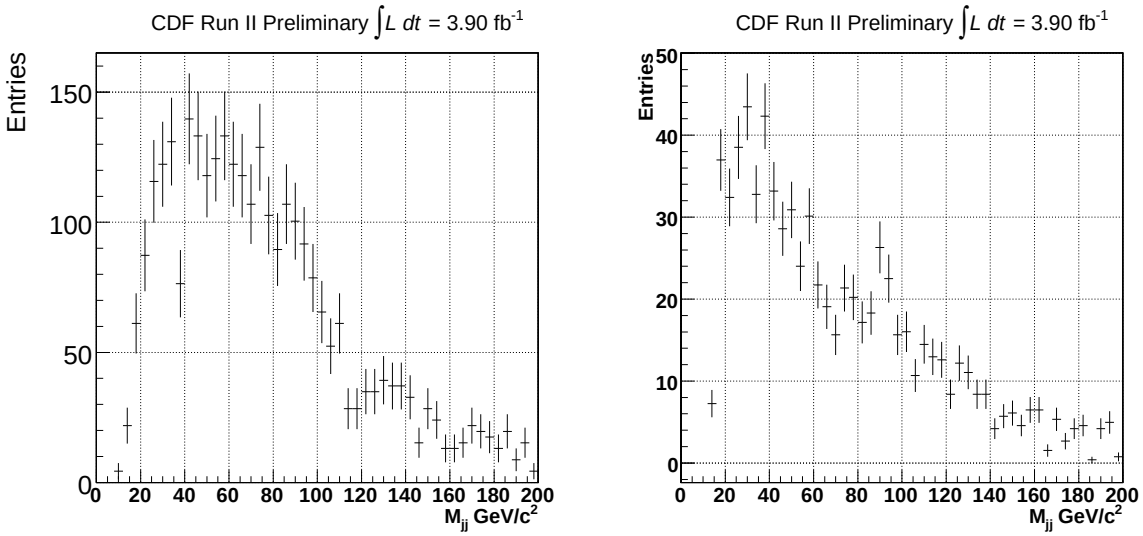

Figure 19: QCD M_{jj} template for electrons (left) and muons (right).

However, as discussed in section 11, the effect of the gaussian constraint on the QCD contribution to the central value of the signal content is negligible.

9.3 Signal Template

The signal template, both for electrons and muons, are obtained from Monte Carlo combinging the WW and WZ templates, whose relative normalizations are fixed by Monte Carlo.
The resulting tempaltes are shown in Fig.20 for electrons (left) and muons (right).

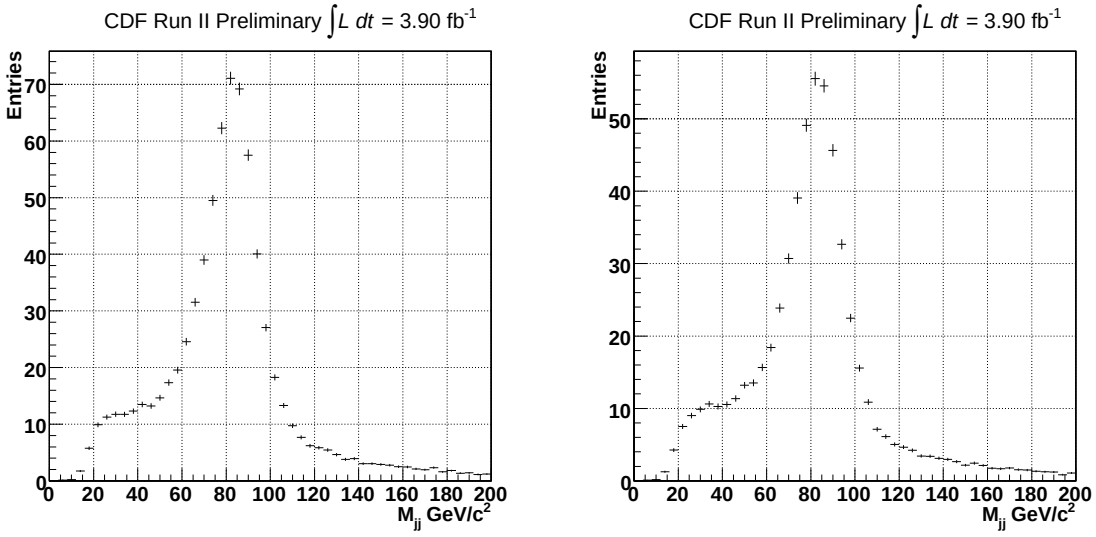

Figure 20: WW/WZ M_{jj} template for electrons (left) and muons (right).

9.4 Fitter Validation

Our fit procedure is valided through pseudo-experiments. We run, independently for electrons and muons, 10000 toy experimets using the previously described signal and background models. The expected content of each component of Tab.6 is used as input of the pseudo-experiment generation.
As shown in Fig.21 and Fig.22, the residual and pull distributions of the estimated number of signal events do not show any deviation form the central vaule used in the generation; moreover, the pull width is compatible with one.
We conclude that our fitting procedure does not introduce any bias in the signal content estimation and the corresponding uncertainty is correctly estimated by MINUIT.

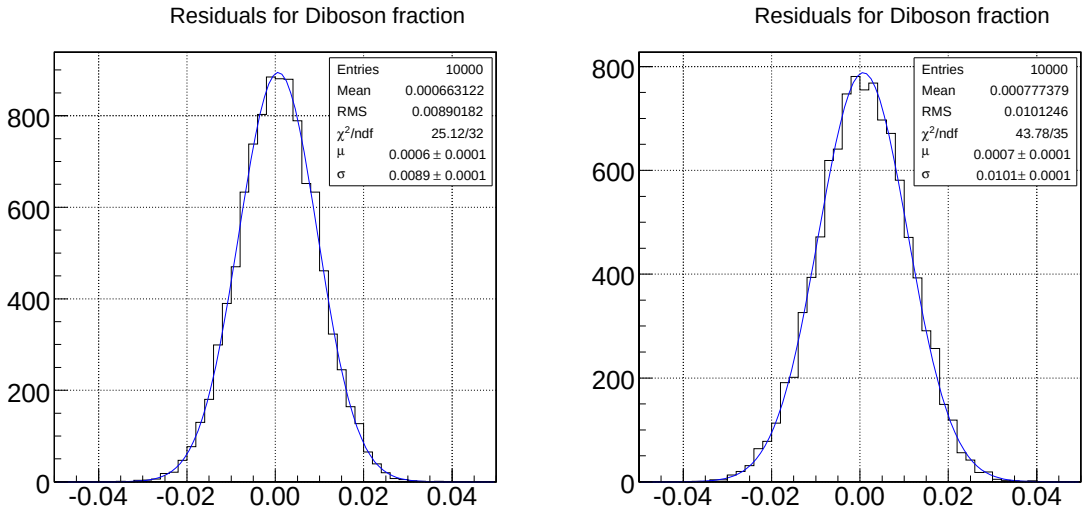

Figure 21: Residual distribution of the Signal content estimator for electrons (left) and muons (right).

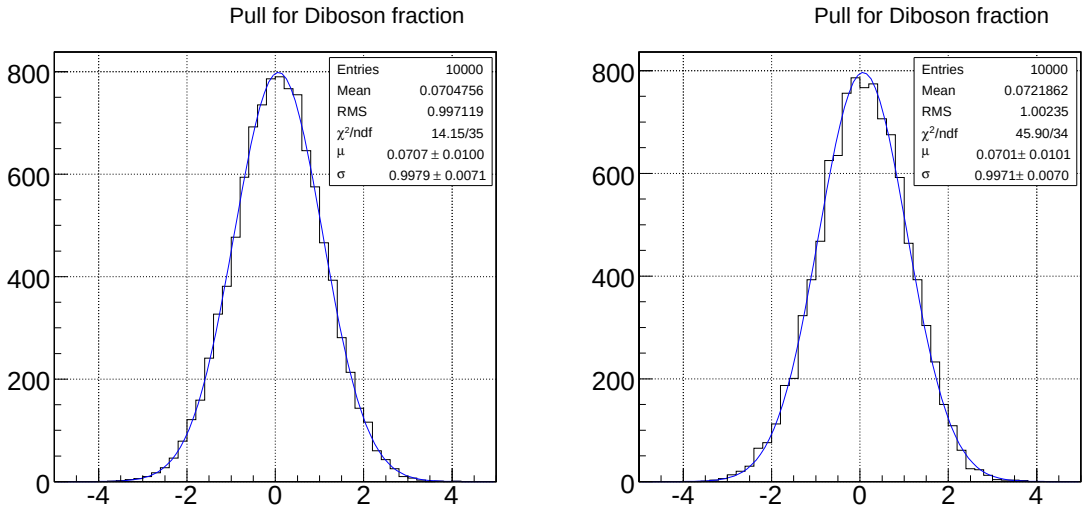

Figure 22: Pull distribution of the Signal content estimator for electrons (left) and muons (right).

9.5 Fit Results on Data

In Fig.23 we show the fit on data for electrons and muons. The estimated fractions are shown in table 7. We estimate 429 ± 177 (stat.) events in the electron sample and 650 ± 149 (stat.) events in the muon sample.
In Fig.25 we show, separately for the two decay channel, the data M_{jj} distribution after background subtraction with Monte Carlo signal normalized to the fit result superimposed. In Fig.26 we show the same plot when the electrons and muons are combined.

	Electron	**Muon**
f_{sig}	0.0227± 0.0094	0.048± 0.011
f_{qcd}	0.083 ± 0.016	0.0428 ± 0.0083
$Total\#Events$	18866 ± 148	13549 ± 122
Observed Total # Events	18905	13573

Table 7: Fit results.

Electron Sample	Total # of Events	f_{qcd}	f_{sig}
Total # Events	1.000	0.016	-0.005
f_{qcd}	0.016	1.000	-0.114
f_{sig}	-0.005	-0.114	1.000
Muon Sample			
Total # Events	1.000	0.002	-0.005
f_{qcd}	0.002	1.000	0.014
f_{sig}	-0.005	0.014	1.000

Table 8: Fit correlation matrices.

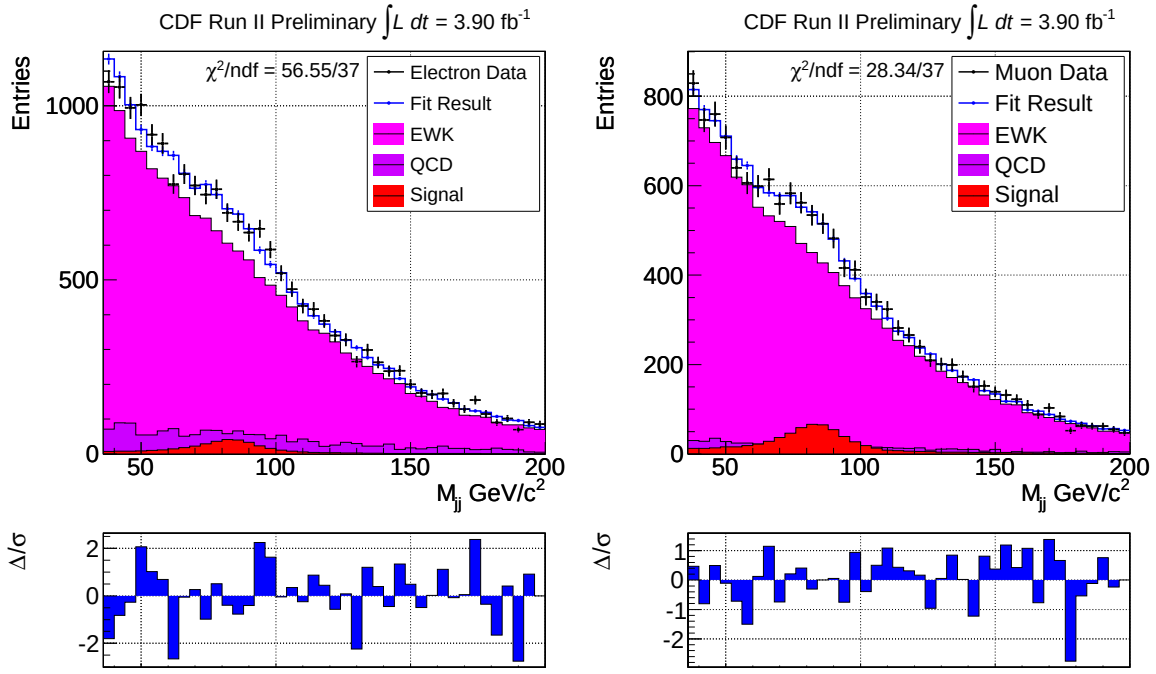

Figure 23: Fit on data for electrons (left) and muons (right). Magenta is EWK, Pink qcd and red is signal. In Blue there's the fit projection and data in black

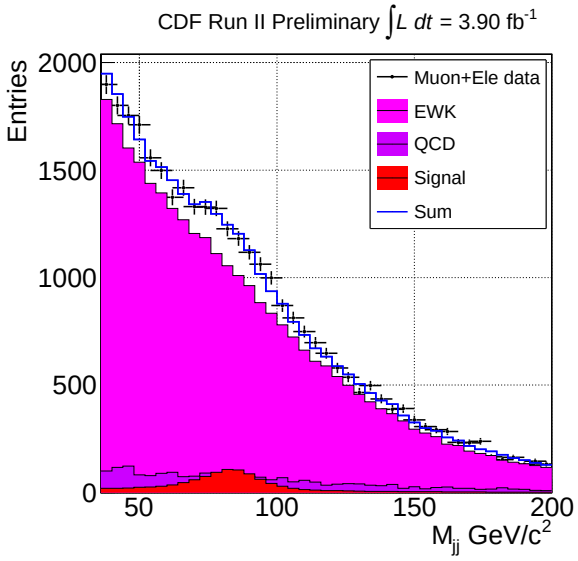

Figure 24: Sum of electron and muons data . Magenta is EWK, Pink qcd and red is signal. In Blue there's the fit projection and data in black

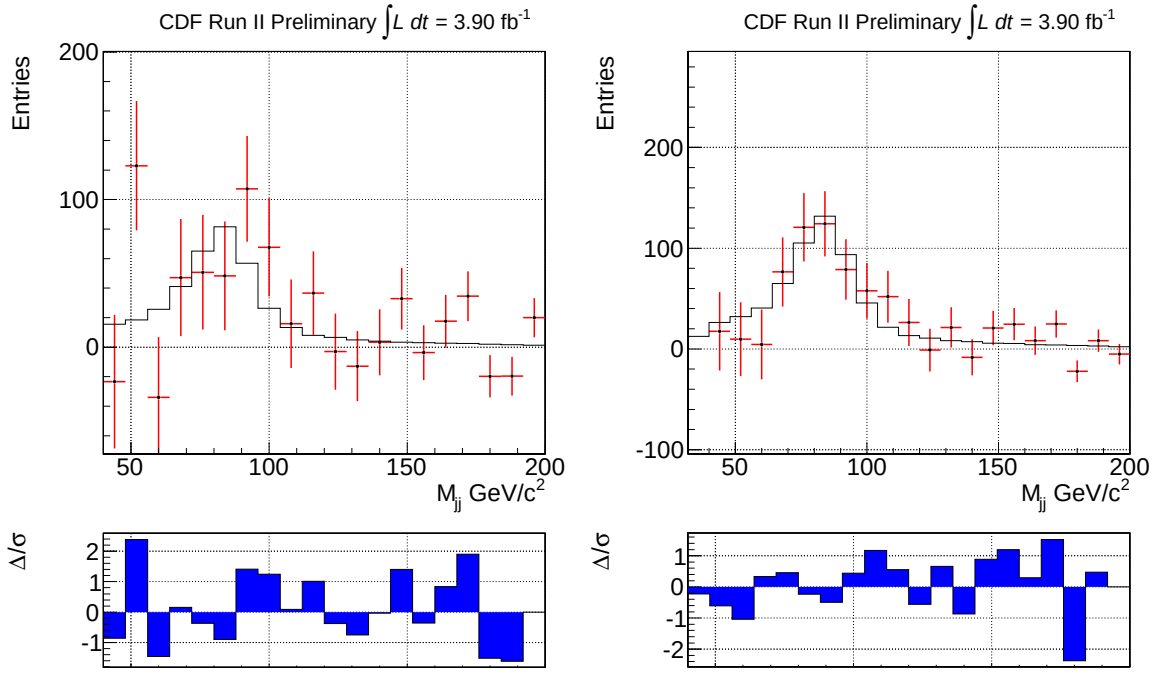

Figure 25: Background subtracted data (points) for electrons (left) and muons (right) superimposed to Monte Carlo signal normalized to the fit result (histogram).

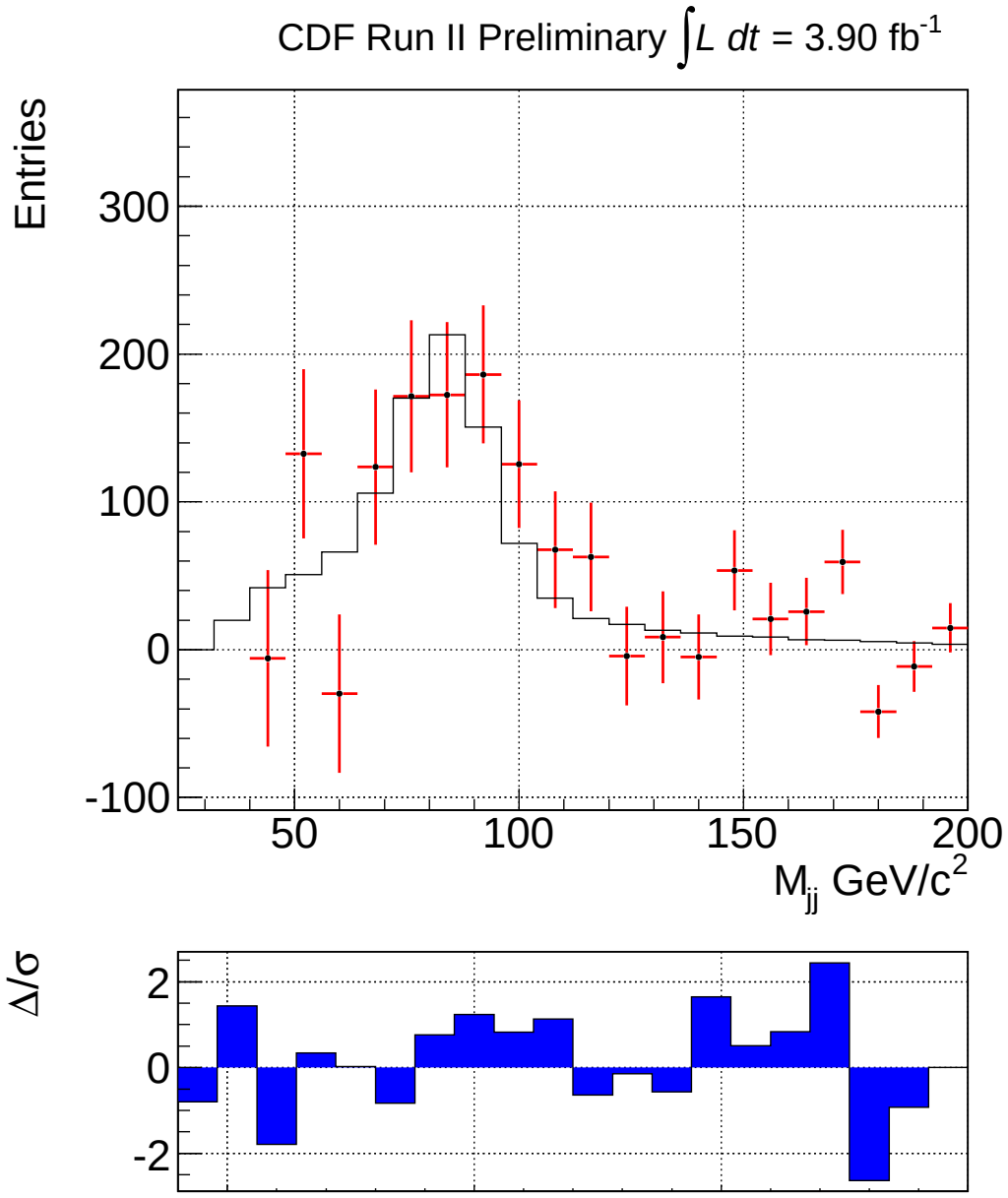

Figure 26: Background subtracted data (points) for muons+electrons superimposed to Monte Carlo signal normalized to the fit result (histogram).

10 Expected Significance

To evaluate the expected significance of our fit on data, we performed 10000 pseudo-experiments. The event content of each component of Tab.6 is used as input of the pseudo-experiment generation.
In Fig.27 we show the distribution of the significance estimators of the signal fraction (defined as $f^{fitted}_{WW/WZ}/\sigma^{fitted}_{WW/WZ}$) for electrons and muons considering the statistical uncertainty only.
We expect a significance of 4.0σ and 3.7σ in the electron and muon sample respectively. A quick combination of the two values gives an expected significance of 5.5σ (statistics only).

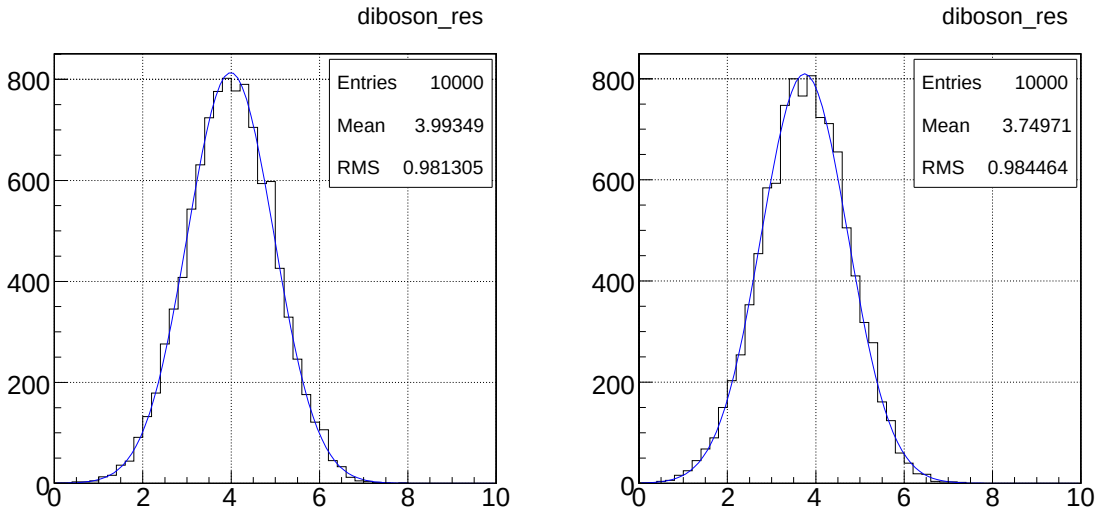

Figure 27: Expected Significance for electrons (left) and muons (right); Statistical uncertainty only.

11 Systematics

We consider two classes of systematics: the systematics affecting signal extraction (i.e. the number of signal events estimated in our data samples) and the additional systematics affecting the signal cross-section.
If not otherwise explitely stated, we estimate the systematics on the signal extraction by generating pseudo-experiment using an alternative template model for each systematic source. The pseudo-experiments are then fitted using the templates used in the main fit on data.
The difference between the central value of the fit on data and the mean of the estimator of the signal content on the alternative pseudo-experiment is taken as systematics on the corresponding source.
Tab.11 shows our systematics results; the total systematics is obtained adding in quadrature each individual contribution. In sections 11.1 and 11.2 we describe in detail how the systematics associated to each source has been evaluated.

	Source	e %	μ %	**e # of Ev.**	μ**# of Ev.**
Signal Extraction	QCD shape	6.4%	4.8 %	28	31
	EWK shape	9.8%	6.6%	42	43
	JES up	5.1%	5.7%	22	37
	JES down	2.8%	1.6%	12	10
	JER	1.4%	1.1 %	6	7
TOTAL		13.1 %	10.1 %	56	65
Cross section	Luminosity	6%	6%	26	39
	Lepton Acceptance	2%	2%	9	13
	ISR more	1.9%	1.4%	8	9
	ISR less	-1.9%	-1.4%	8	9
	FSR more	0.5%	3%	2	19
	FSR less	-0.5%	-3%	2	19
	PDF	2.0%	2.0 %		13
TOTAL		14.8 %	12.8%	63	83

Table 9: Systematics uncertainties.

11.1 Signal Extraction

For signal extraction we consider the following systematics sources:

- **Jet Energy Scale**

  The Jet Energy Scale systematics is estimated varying the JES by $\pm 1\sigma$ with respect to its central value. Since the JES does not affect the QCD component,

the alternative tempaltes are generated for the EWK and signal only.
Two different templates corresponding to JES $+1\sigma$ and JES -1σ are obtained for the EWK and the signal components separately for electrons and muons. The new templates are shown in Fig.28 and 29. The corresponding systematic is evaluated to be JES $+1\sigma = 5.1\%$ and JES $-1\sigma = 2.8\%$ for electrons and $+1\sigma = 5.7\%$ and JES $-1\sigma = 1.6\%$ for muons.

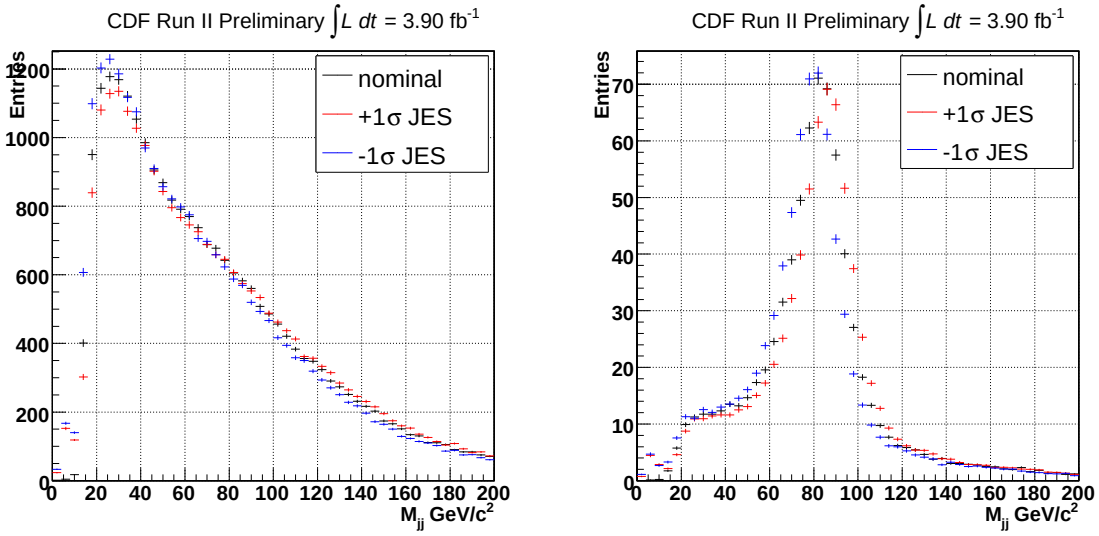

Figure 28: JES $\pm 1\sigma$ templates for EWK (left) and signal in the electron sample.

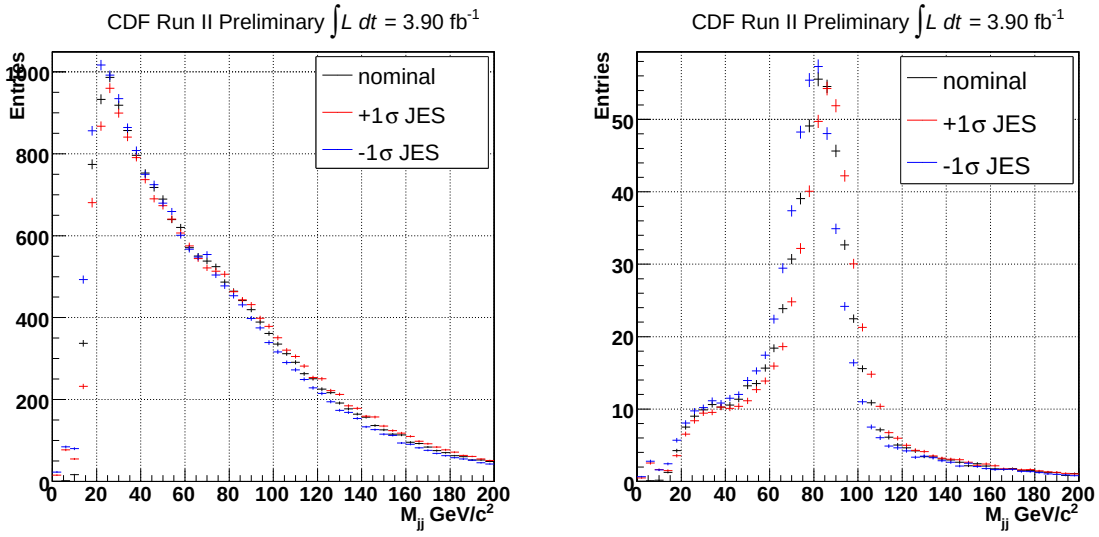

Figure 29: JES $\pm 1\sigma$ templates for EWK (left) and signal in the muon sample.

- **Jet Energy Resolution**

  The dijet signal and ewk template are smeared according to the uncertainty on the jet energy resolution of $0.03 \pm 1.7/E_T$ [7]. The alternative template obatined by smearing (Fig.30) are then used to asses the corresponding systematics that is evaluated to be 1.4% for electrons and 1.1 % for muons.

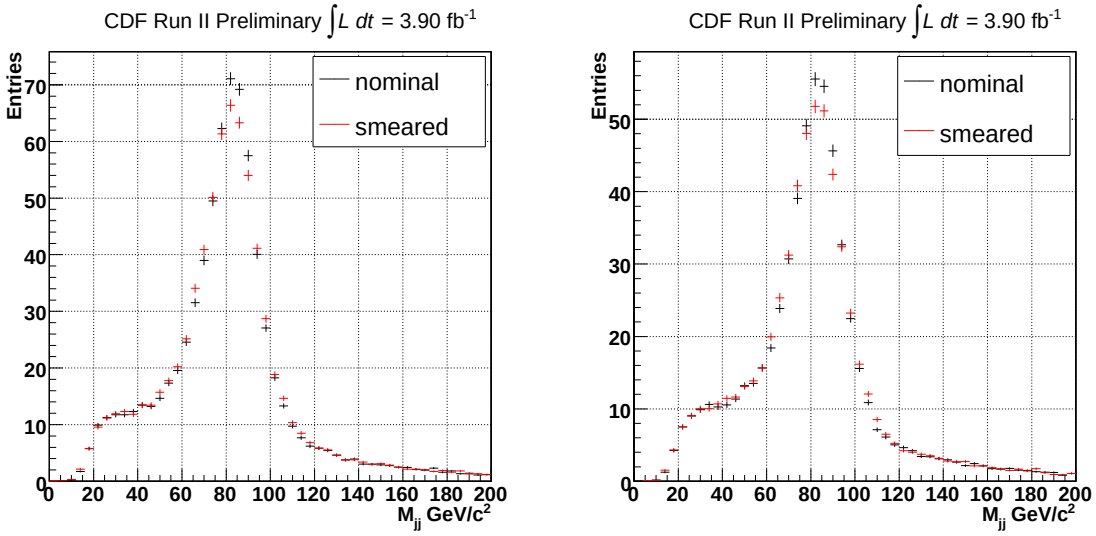

Figure 30: JER smeared templates for signal in electrons (left) and muon sample.

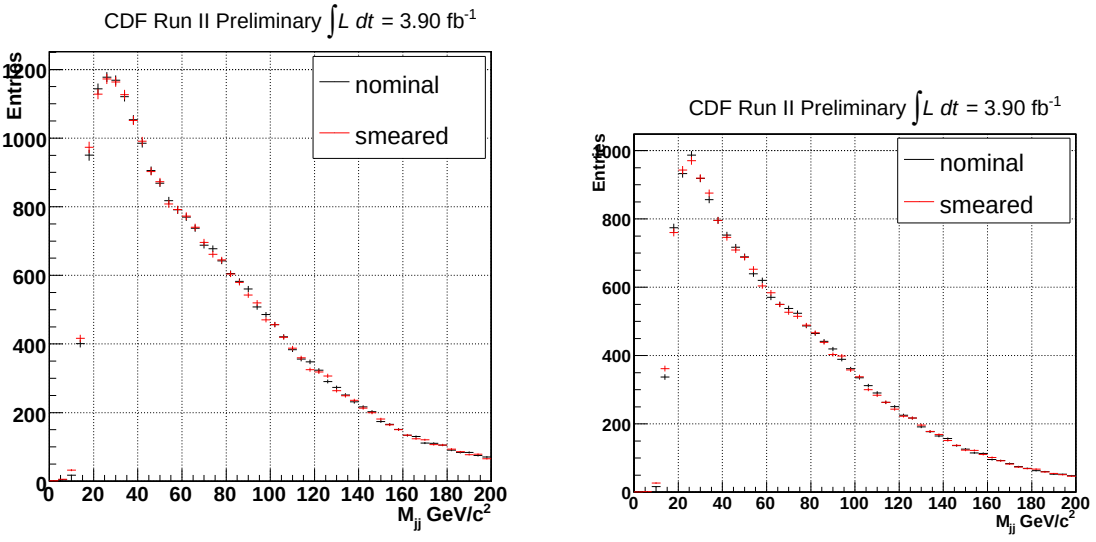

Figure 31: JES smeared templates for EWK (left) and signal in the muon sample.

- **Electroweak Shape**

  Having already considered JES and JER as possible sources of uncertainty on the shape of the EWK template, the only remaining effect might be due to mismodeling of the involved physics processes.
  The main contribution to the EWK component arises from $W + jets$ events. For this reason, we investigate the effect of different relative composition of the $W + np$ processes.
  In particular, we generated a new EWK template (again, separately for electrons and muons) removing the $W+(n > 3p)$ and $W+HF$ processes; removing $W+np$ with any $n \leq 3$ would be too unrealistic and we decided to consider as alternative templates the ones obtained with $W + (n \leq 3p)$ (shown in Fig.32).
  The corresponding systematic is evaluated to be 9.8% for electrons and 6.6 % for muons.

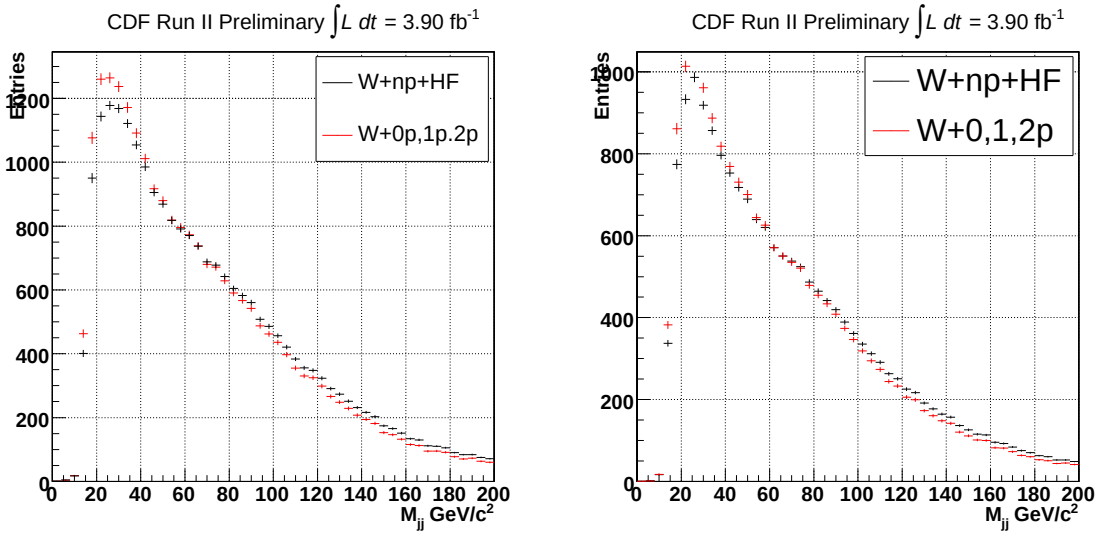

Figure 32: EWK template used in systematic evaluation overimposed to the main fit template; electrons (left), muons (right).

- **QCD Shape and Normalization**

  The systematic associated with the QCD M_{jj} shape component is evaluated using different QCD templates. The alternative templates are obtained, separately for electrons and muons, considering data events with $Iso > 0.2$ and $Iso > 0.4$ respectively.
  In Fig.33 we overimpose the template used in the main fit to the ones used in the systematics for electrons (left) and muons (right).
  The corresponding systematic is evaluated to be 6.4% for electrons and 4.8% for muons.

In addition, the QCD contribution is gaussian-constrained in our fit procedure. However, if we remove the constraint and let the QCD normalization free do be determined by the fit (on data), we estimate a fraction of 0.049 ± 0.013 for muons and 0.025 ± 0.009 for electrons. The values are almost identical to our central results; we then decided to consider the associated systematics negligible.

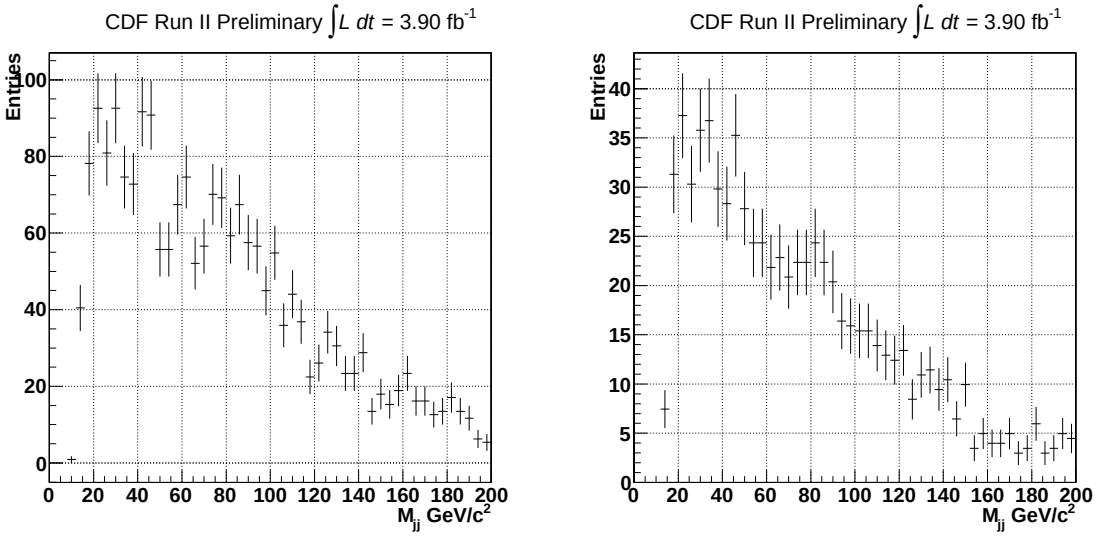

Figure 33: QCD template used in systematic evaluation overimposed to the main fit template; electrons (left), muons (right).

11.2 Cross-section

In addition to the signal extraction systematics, for the cross-section measurement we consider also the following sources:

- **Luminosity:** The standard 6% systematics is considered.
- **Lepton Acceptance:** We quote a 2% systematics on the lepton acceptance.
- **ISR/FSR:** We take the sample of higgs produced in association with W with ISR and FSR changed since there are no available MC sample for our channel and scale the E_T of jets by 80./120. Then we take the difference in acceptance between the sample with more ISR and less ISR divided by two. We do the same for the FSR systematics.
- **PDF:** We quote the same systematics used in $WH \to l\nu b\bar{b}$ that was found to be 2.0% [8] (the worst case with double tag).

12 Constraining the JES

We also tried to allow the jet energy scale to float in the extraction fit. For this purpose we performed an unbinned maximum likelihood fit to our data. In this cross-check, for simplicity we decided to perform one single combined fit to the electron an muon sample together.
Signal template is parameterized as the sum of two gaussians and a first order polinomial. The mean of the main gaussian (the one describing the signal at the peak) is multiplied by a scale factor that is left free to be determined by the fit. This scale factor is the multiplicative correction to be applied to our expected JES and, if significantly different from one, it provides evidence of a different JES in data.
The EWK and QCD template are not parameterized and the corresponding normalized histograms (the same used in the main fit) are used as probability density functions.
In Tab. 10 we show the results of the new fit and in Fig.34 its projection.
The fitted scale factor is consistent with one at $\sim 1\sigma$.

	Value found
f_{sig}	0.0354 ± 0.0069
f_{qcd}	0.0543 (constrained)
JES	1.037 ± 0.035

Table 10: JES constraining.

13 Acceptance

We might argue that since we are using events with $p_T(W) > 40GeV/c$ we should quote the cross section for those events. To do this, we calculate the ratio between the number of events that pass our cuts at quark level including the cut of $p_T > 40GeV/c$ and the number of events at quark level with $p_T > 0GeV/c$ (Tab. 11). The formula used for quoting the cross section is:

$$\sigma^{40}_{measured} = \frac{N_{obs} \cdot \sigma^{40}_{theory}}{N_{MC}}$$

where N_{obs} is the number of events in data, σ_{theory} is the standard model cross section ($16.1 \pm 0.9pb$), N_{MC} is the number of events of MC (corrected for all efficiency and acceptance). We calculate σ^{40}_{theory} form the MC as:

$$\sigma^{40}_{theory} = \sigma^{0}_{theory} * \frac{N_{pt>40}}{N_{pt>0}}$$

where $N_{pt>0}$ is the number of events at quark level with $p_T > 0GeV/c$ and $N_{pt>40}$ is the number of events at quark level with $p_T > 40GeV/c$,σ^{0}_{theory} is the theoretical cross

section . We can now quote the cross section (for $p_T > 40GeV/c$) $5.3 \pm 2.3(stat.) \pm 1.0(syst.)$ pb for electrons and $10.1 \pm 2.6(stat.) \pm 1.9(syst)$ pb for muons, respectively. The combined result for $p_T > 40GeV/c$ is $\sigma^{40}_{WW/WZ} = 7.4 \pm 1.7$(stat.) $\pm$ 1.4 (syst.) pb.

	Electron	**Muon**
$p_T > 0GeV/c$	2557	2276
$p_T > 40GeV/c$	1329	1158

Table 11: Acceptance. The MC statistical error is negligible.

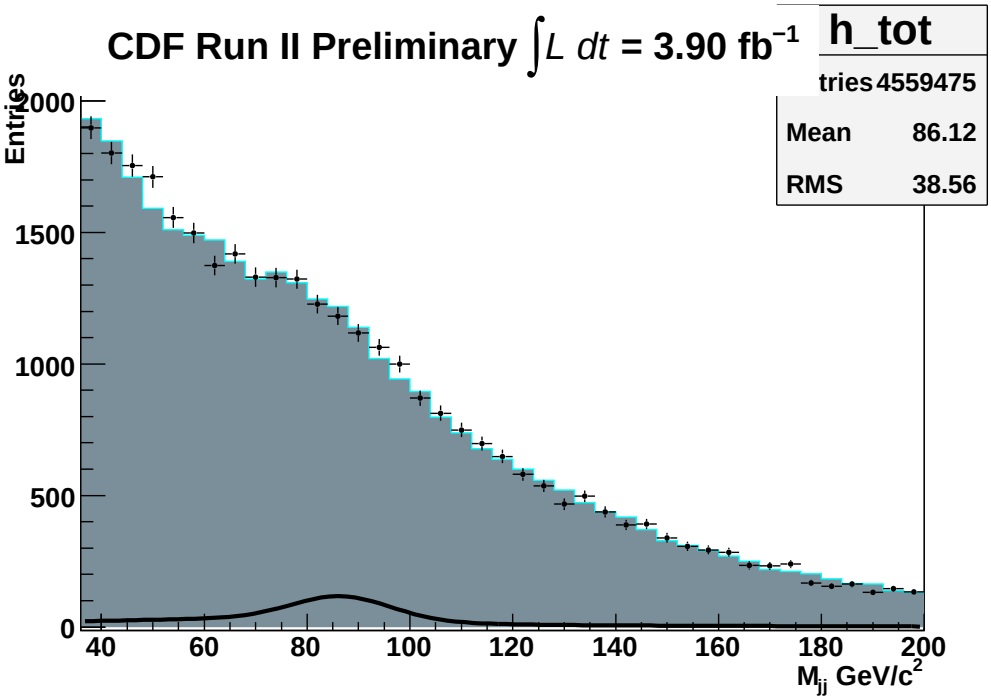

Figure 34: Fit to data with JES floating, in black is signal.

14 Final Results

In a data sample corresponding to 3.9 fb^{-1} of integrated luminosity of high p_T muons and electrons, we performed a search for $WW/WZ \to l\nu jj$ processes.
Using a fit to the invariant mass distribution M_{jj} we estimate 428 ± 177 (stat.) ± 56 (syst.) events in the $WW/WZ \to e\nu jj$ sample and 650 ± 149 (stat.) ± 66 (syst) events in the $WW/WZ \to \mu\nu jj$ sample that leads to a cross section of 10.3 ± 4.2 (stat.) ± 1.7 (syst.) pb for electrons and 19.5 ± 4.7 (stat.) ± 2.8(syst) pb for muons, respectively.
Combining the two decays, we estimate a total of 1079 ± 232 (stat.) ± 86 (syst.) $WW/WZ \to l\nu jj$ events, corresponding to a significance of 4.4 σ. Finally, we measure $\sigma_{WW/WZ} = 14.4 \pm 3.1$(stat.) ± 2.2 (syst.) pb.

	Electron	**Muon**	**Combined**
# WW/WZ	428 ± 177 ± 56	650 ± 149 ± 66	1079 ± 232 ± 86
$\sigma_{WW/WZ}$ (pb)	10.3 ± 4.2 ± 1.7	19.5 ± 4.7 ± 2.8	14.1 ± 3.1 ± 2.3

Table 12: Final Results.

References

[1] G. Flanagan, J Freeman, S. Pronko, V. Rusu, CDF Note 9736.

[2] T.Spreitzer *et al.*,"Electron Identification in Offline Release 6.1.2", CDF Note 7950.

[3] J. Adelman *et al.*, Method II For You, CDF Note 9185.

[4] B. Cooper, A. Messina, "Estimation of the Background to W e + n Jet Events", CDF note no. 6636.

[5] D.Amidei *et al.*,"First Measurements of Inclusive W and Z Cross Sections from Run II of the Tevatron Collider", Phys. Rev. Lett. 94, 091803 (2005).

[6] N. D. Gagunashvili, Proceedings of the Conference on Statistical Problems in Particle Physics, Astrophysics and Cosmology, 43-44, 12-15 September, 2005, Oxford, Imperial College Press, London, 2006.

[7] F. Canelli *et al.*, CDF Note 7856.

[8] J. Dittman *et al.*, CDF Note 9401.